RESEARCH ARTICLE

NANO · MICRO small
www.small-journal.com

Long-Lasting, Transparent Antibacterial Shield: A Durable, Broad-Spectrum Anti-Bacterial, Non-Cytotoxic, Transparent Nanocoating for Extended Wear Contact Lenses

Nahyun Park, Chae-Eun Moon, Younseong Song, Sang Yu Sun, Ji-Min Kwon, Sunghyun Yoon, Seonghyeon Park, Booseok Jeong, Jemin Yeun, Joseph Michael Hardie, Jun-ki Lee, Kyoung G. Lee, Yong Woo Ji,* and Sung Gap Im**

The increasing incidence of serious bacterial keratitis, a sight-threatening condition often exacerbated by inadequate contact lens (CLs) care, highlights the need for innovative protective technology. This study introduces a long-lasting antibacterial, non-cytotoxic, transparent nanocoating for CLs via a solvent-free polymer deposition method, aiming to prevent bacterial keratitis. The nanocoating comprises stacked polymer films, with poly(dimethylaminomethyl styrene-*co*-ethylene glycol dimethacrylate) (pDE) as a biocompatible, antibacterial layer atop poly(2,4,6,8-tetramethyl-2,4,6,8-tetravinylcyclotetrasiloxane) (pV4D4) as an adhesion-promoting layer. The pD6E1-*grafted* (*g*)-pV4D4 film shows non-cytotoxicity toward two human cell lines and antibacterial activity of >99% against four bacteria, including methicillin-resistant *Staphylococcus aureus* (MRSA), an antibiotic-resistant bacteria and *Pseudomonas aeruginosa*, which causes ocular diseases. Additionally, the film demonstrates long-lasting antibacterial activity greater than 96% against MRSA for 9 weeks in phosphate-buffered saline. To the best knowledge, this duration represents the longest reported long-term stability with less than 5% decay of antibacterial performance among contact-killing antibacterial coatings. The film exhibits exceptional mechanical durability, retaining its antibacterial activity even after 15 washing cycles. The pD6E1-*g*-pV4D4-coated CL maintains full optical transmittance compared to that of pristine CL. It is expected that the unprecedentedly prolonged antibacterial performance of the coating will significantly alleviate the risk of infection for long-term CL users.

1. Introduction

Contact lenses (CLs) that undergo continuous use inevitably accrue mechanical damage on their surfaces, which may act as a favorable environment for bacterial keratitis (BK). This phenomenon poses a significant public ocular health issue, accounting for approximately up to 2 million cases of visual impairment annually.[1] In severe cases, BK results in vision impairment and even total blindness, necessitating the use of antibiotics as a counteracting agent.[2] However, due to the need for multiple periodic doses, the antibiotic treatment entails potential risks including cytotoxicity, tissue damage, and promotion of antibiotic-resistant bacterial strains.[3] To date, BK is primarily attributed to various bacteria including *P. aeruginosa*,[4] *S. aureus*,[5] and methicillin-resistant *Staphylococcus aureus* (MRSA). [5] Therefore, it is imperative to develop a long-lasting antibacterial surface coating method with chemical stability and mechanical durability to prevent BK.[1b]

The rise of reusable CLs, with extended periods ranging from 2 weeks to 2 years, presents an increased risk of bacterial infection due to improper maintenance,

N. Park, Y. Song, S. Yu Sun, S. Yoon, S. Park, B. Jeong, J. Yeun, S. G. Im
Department of Chemical and Biomolecular Engineering
Korea Advanced Institute of Science and Technology
291 Daehak-ro, Daejeo, Yuseong-gu 34141, Republic of Korea
E-mail: sgim@kaist.ac.kr

C.-E. Moon, J.-M. Kwon, J.-ki Lee, Y. W. Ji
Institute of Vision Research
Department of Ophthalmology
Yonsei University College of Medicine
Seoul 03722, Republic of Korea
E-mail: lusita30@yuhs.ac

The ORCID identification number(s) for the author(s) of this article can be found under https://doi.org/10.1002/smll.202405635

DOI: 10.1002/smll.202405635

Y. Song, J. M. Hardie
Division of Engineering in Medicine
Department of Medicine
Brigham and Women's Hospital and
Harvard Medical School
Boston, Massachusetts 02139, USA

K. G. Lee
Division of Nano-Bio Sensors/Chips Development
National NanoFab Center (NNFC)
291 Daehak-ro, Daejeon, Yuseong-gu 34141, Republic of Korea
E-mail: kglee@nnfc.re.kr

Y. W. Ji
Department of Ophthalmology
Yongin Severance Hospital
Yonsei University College of Medicine
Yongin-si 16995, Republic of Korea

underscoring the necessity for antibacterial coatings.[6] To apply antibacterial coatings to reusable CLs, it is crucial to consider the following factors: 1) chemical stability, 2) mechanical durability, and 3) optical transparency. In the corneal environment or contact lens solution containing various ionic species, the poor stability of the coating – especially in a saline environment – can provoke antibacterial coating damage, such as cracking, delamination, or dissolution of the coating layer,[7] which may result in leaching of antibacterial functionalities therefrom.[8] In the event of release or leaching of antibacterial moieties from the coating, toxicity risks can also arise, highlighting the importance of the chemical stability of the coating.[9] Given the potential damage incurred during cleaning and repeated use of CLs, the mechanical durability of the coating is one of the most crucial factors to be considered.[7a] For successful application in contact lenses, it is essential to select materials with low absorbance in the visible spectrum and refractive indices closely matching those of lens materials to maintain full optical transparency. Therefore, it is critical to develop an antibacterial coating that is durable, non-cytotoxic, and transparent.[10]

Many previous studies have aimed to develop coatings with long-lasting antibacterial effects, based on two primary mechanisms: the release of antibacterial agents and contact-killing mechanisms. Despite the extensive research, the application of these antibacterial coatings to CLs remains challenging.[8,11] The release of antibacterial agents, such as Ag^+ ions, antimicrobial peptides, and small molecule antibiotics,[8,11a–h] has proven effective in eradicating bacteria; however, there are limitations, including potential cytotoxicity,[9,12] limited loading capacity,[8,9,11c] and the risk for the bacteria to acquire antibiotic resistance.[3,13] While the use of quaternary ammonium compounds (QACs)[11f] and antimicrobial peptide (AMP) coatings[2a,11i] could maintain antibacterial activity for contact-killing on a substrate, QACs and AMPs applied to the substrate suffered from poor adhesion, especially in the salt ion-rich environments.[14] Furthermore, the QAC-based method does not ensure long-lasting antibacterial properties due to the coating degradation and release of antibacterial substances from the substrate.[15]

In this study, we propose a novel, long-lasting antibacterial coating directly applicable to CL surfaces with outstanding mechanical and chemical durability, especially in the corneal environment. These lenses are coated directly with a stacked polymer film, featuring a robust antibacterial surface. The polymer comprises two layers: the bottom layer consists of poly(2,4,6,8-tetramethyl-2,4,6,8-tetravinylcyclotetrasiloxane) (pV4D4), serving as an adhesion-promoting layer to provide strong surface adhesion as well as mechanical passivation for the CL, while the top layer grafted on the adhesion-promoting layer is a copolymer synthesized from two monomers, dimethylaminomethyl styrene (DMAMS) and ethylene glycol dimethacrylate (EGDMA) to possess antibacterial activity as well as non-cytotoxicity. All the polymer layers are synthesized via a vapor-phase method, initiated chemical vapor deposition (iCVD) process. The process ensures conformal modification of 3D CL structure in a solvent-free manner at room temperature, which ensures damage-free modification of the CL surface. The deposition process preserves the full transparency of the CLs in the whole visible range.[16] The copolymer film also demonstrates outstanding biocompatibility and strong antibacterial performance.[17] The p(DMAMS-*co*-EGDMA)-*g*-pV4D4-coated CLs demonstrate remarkable chemical stability, maintaining antibacterial performance in aqueous solution with high salt ion concentration for at least more than 9 weeks. The unprecedentedly prolonged antibacterial performance of the developed anti-bacterial coating is expected to reduce the risk of infection for long-term CL users and can be extended to various medical device applications.

2. Result and Discussion

2.1. Design Strategy and Synthesis of the Long-Lasting Anti-Bacterial Polymer Films

Human hands are a known source of bacteria and are considered high-potential vectors for causing BK on the CL surfaces. (**Figure 1a**). We expect that the CL surface modified with the long-lasting anti-bacterial coating can eradicate bacteria even when worn, thus minimizing the occurrence of BK.

To develop a long-lasting antibacterial polymer thin film for reusable CL, we designed the composition of the anti-bacterial coating to satisfy the following criteria: 1) effective antibacterial performance to prevent bacterial infection on the CLs, 2) non-cytotoxicity to minimize corneal side effects, and 3) long-lasting antibacterial activity in physiological aqueous environments with high concentration of salt ions, ensuring chemical stability and mechanical durability to prevent film failure during wear.

In Figure 1b, an organosilicon adhesion-promoting layer, pV4D4 was introduced to enhance the adhesion of the antibacterial coating to the target surfaces via the iCVD process.[18] This layer adheres strongly to various substrate materials,[19] and to the CL surface as well. The adhesion-promoting effect of the pV4D4 layer is primarily attributed to the residual vinyl groups present in pV4D4. The multiple vinyl groups in the pV4D4 serve as cross-linkable anchoring sites, allowing for the grafting of various functionalities onto polymer brushes, by forming strong covalent bonds with the overlaying layers.[18–19] We introduced a copolymer layer, p(DMAMS-co-EGDMA), or pDE[20] to achieve superior anti-bacterial activity and non-cytotoxicity grafted on top of the pV4D4 layer. Achieving both antibacterial efficacy and biocompatibility on the pDE surface is a crucial goal of this study. The antibacterial performance of the pDE surface primarily stems from a "contact-killing" mechanism, driven by the protonation of the DMAMS moiety under physiological conditions, which results in the surface becoming cationic.[17b,c,20] These positive charges interact with the anionic lipids in bacterial cell membranes, particularly phosphatidylglycerol, leading to membrane disruption, leakage of intracellular contents, and eventual bacterial cell death. However, this electrostatic interaction, while effective against bacteria, could also pose a risk to mammalian cells. The key difference lies in the membrane composition: bacterial membranes are rich in anionic lipids, such as phosphatidylglycerol, making them particularly susceptible to electrostatic interactions, whereas mammalian cell membranes predominantly contain neutral lipids like phosphatidylcholine and sphingomyelin in their outer layers.[21] This difference in membrane composition led us to hypothesize that by precisely controlling the surface charge through adjustments to the DMAMS composition, we could selectively target bacterial cells while minimizing cytotoxic effects on mammalian cells. Incorporating pEGDMA as a

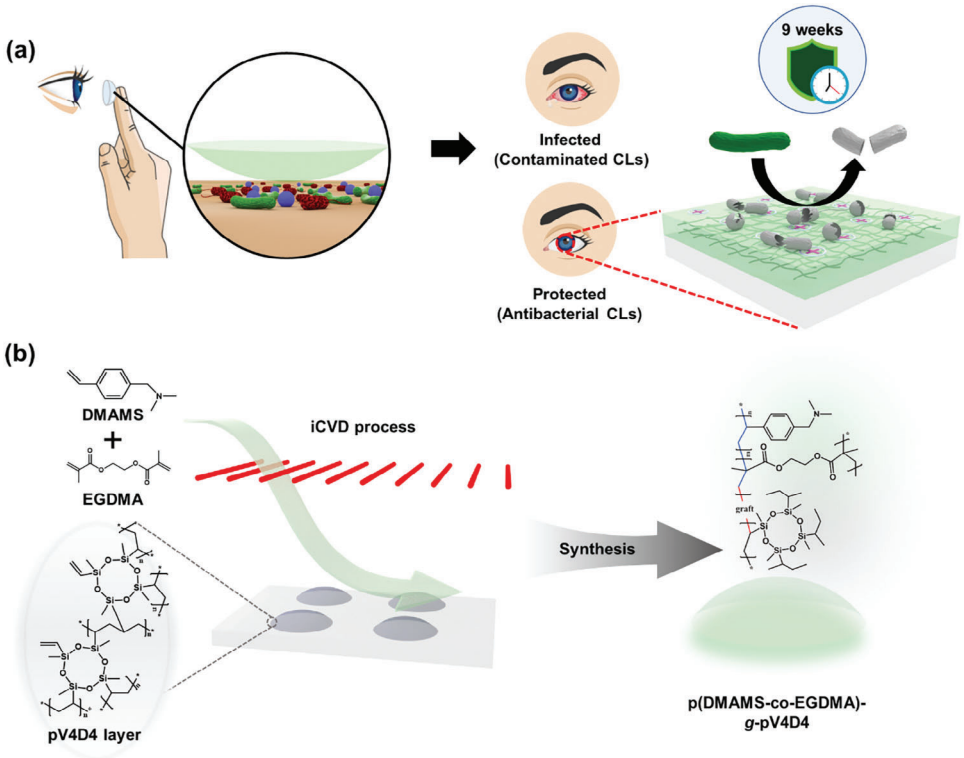

Figure 1. A schematic illustration of a) antibacterial CLs to eradicate broad-spectrum bacteria and prevent bacterial keratitis compared to pristine CLs and b) the synthesis of long-lasting anti-bacterial and non-cytotoxic copolymer film with chemical stability and mechanical durability via an iCVD process.

biocompatible cross-linker further supported this balance, leading to the successful development of a polymeric film that is both effective against bacteria and safe for mammalian cells.[22] Consequently, a pDE-*g*-pV4D4 layer synthesized via the iCVD process enhances chemical stability and mechanical durability in an aqueous saline solution similar to a corneal environment.

2.2. Characterization of the pDE Film

To determine the optimal conditions for balancing antibacterial activity and biocompatibility, pDE copolymers were synthesized using the iCVD process with three distinct compositions—pD8E1, pD6E1, and pD4E1 – utilizing DMAMS to EGDMA input flow ratios of 8:1, 6:1, and 4:1, respectively. The 8:1 ratio was chosen for its superior antibacterial activity, the 4:1 ratio for its high biocompatibility, and the 6:1 ratio as a compromise that balances both properties effectively. These ratios were expected to reflect key points where the interaction between antibacterial efficacy and biocompatibility is most significant. Fourier-transform infrared spectroscopy (FT-IR) and X-ray photoelectron spectroscopy (XPS) analyses were conducted to characterize the composition of each copolymer. As shown in **Figure** 2a, the FT-IR spectra of pDE copolymers exhibited distinct peaks at 1722 cm^{-1} and at 2765 cm^{-1} representing the carbonyl group in EGDMA and the tertiary amine moiety in DMAMS, respectively. With an increase in the flow ratio of DMAMS, the intensity of the carbonyl peak decreased, while the intensity of the tertiary amine moiety peak gradually increased. This result demonstrated successful adjustment of the pDE copolymer composition through the iCVD process. In the XPS spectra, an increase in the DMAMS flow rate led to a higher XPS N1s peak intensity and a decrease in the O1s peak intensity (Figure 2b). Subsequently, the DMAMS:EGDMA surface compositions for pD8E1, pD6E1, and pD4E1 surfaces were determined as 1.8:1, 1.3:1, and 0.8:1, respectively, based on the quantitative XPS analysis (Figure 2c; Tables S1–S2, Supporting Information).

Protonation of the tertiary amine moiety of DMAMS is a crucial process to convert the amine group to a positively charged QAC, thus imparting antibacterial properties to the pDE films. We exposed the pDE film to a pH 7.4 phosphate-buffered saline (PBS) solution, mimicking physiological conditions,[7a] and measured the protonation through high-resolution XPS scans. In Figure S1a–f (Supporting Information), the N1s spectra of pD8E1, pD6E1, and pD4E1 films showed a significant rise in the peak intensity at ≈401 eV after incubation in PBS solution, indicating the formation of the QACs. Figure 2d shows zeta-potential values of each film in an aqueous environment. As the ratio of DMAMS in the pDE films increased, the zeta-potential value also notably increased from 6.0 to 36.7 mV, showing a positively charged surface was induced in the pDE films in the aqueous environment.

2.3. Anti-Bacterial Performance and Cytotoxicity of pDE Thin Film

To assess the antibacterial performance, *Staphylococcus aureus* (*S. aureus*) was selected as a representative target ocular pathogen for

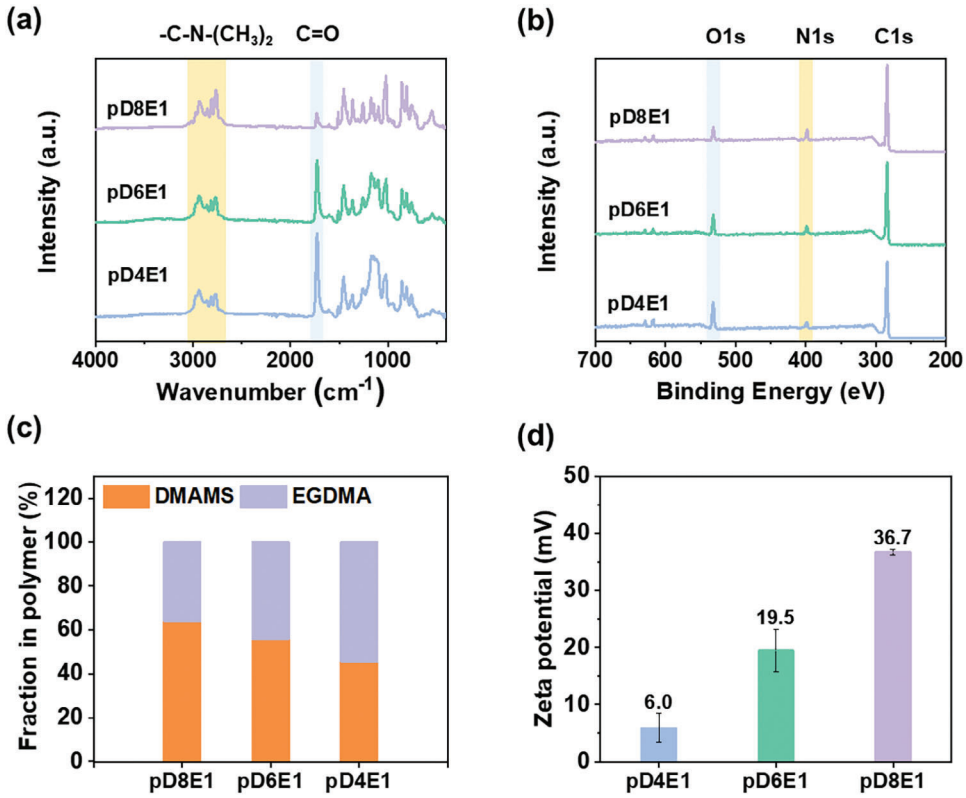

Figure 2. Synthesis and characterization of the pDE films a) FT-IR spectra, and b) XPS survey scan spectra of pD8E1 (light purple), pD6E1 (green), and pD4E1 (light blue) polymers, respectively. c) Fraction of DMAMS and EGDMA in each copolymer after XPS analysis. d) Zeta potential result of pDE films. Error bars indicate standard deviation ($n = 3$).

corneal infections.[23] *S. aureus* cultures (10^5 CFU mL^{-1}) were individually inoculated onto the pristine and pDE-coated CLs and left in contact for 2 h. Subsequently, a colony assay was performed using the samples from both CLs and the bacteria solution (**Figure 3a**). The pristine CL was surrounded by numerous bacterial colonies, while on the CLs coated with pD8E1 and pD6E1, practically no bacterial colonies were detected. For the pD4E1-coated CL, mild to moderate colony growth was detected. The same trend was also observed for the bacteria solution retrieved from each CL (lower images in Figure 3a). In Figure 3b, pD8E1 and pD6E1 copolymer films provided exceptional antibacterial performance, achieving antibacterial efficiencies greater than 99% against *S. aureus* within a 2 h incubation period. In contrast, pD4E1 demonstrated a relatively lower antibacterial efficiency of 71%. The negative control without antibacterial coating exhibited no antibacterial activity. The antibacterial efficiency against *S. aureus* substantially improved with increasing tertiary amine content of DMAMS in the copolymer due to an increased number of protonated amine moieties in the aqueous environment (Table S3, Supporting Information).

A cytotoxicity assay was performed using normal human dermal fibroblasts (NHDFs) as representative cells to simulate potential contact between the antibacterial coatings and human skin, particularly when CLs are worn.[24] NHDFs (5×10^4 cells/well) were seeded onto pDE-coated Petri dishes and cultured for 1 day in vitro (DIV), followed by live/dead fluorescence microscopic analysis to evaluate cell viability on each surface. In Figure 3c, pD8E1 exhibited only minimal green fluorescence and a relatively large amount of red fluorescence, indicating cytotoxic properties, causing cell death or impairment of cellular functions.[22,25] In contrast, the pD6E1 and pD4E1 copolymers showed excellent remaining cell viability of over 99%, comparable to that of the positive control, tissue culture on polystyrene (TCPS) (Figure 3d). These properties can be attributed to the biocompatible EGDMA moiety in the copolymers, diluting the tertiary amine moiety in DMAMS.[10,20] According to ISO-10993-5,[26] relative cell viability exceeding 80% is considered non-cytotoxic for medical devices. Consequently, the pD6E1 and pD4E1 films exhibited non-cytotoxicity for the NHDFs. Therefore, due to its exceptional antibacterial performance as well as non-cytotoxicity, the pD6E1 film was chosen as the optimized composition for application in CLs.

2.4. Characterization and Application of pD6E1-*g*-pV4D4 Film to CL

Following the deposition of pV4D4 onto the CL surface as an adhesion layer, the antibacterial pD6E1 layer was subsequently deposited. FT-IR spectroscopy was employed to analyze the synthesis of pD6E1-*g*-pV4D4.[20] As depicted in **Figure 4a**, the peak at 1070 cm^{-1} (highlighted in gray), representing the asymmetric Si—O—Si stretching peak from the cyclic siloxane ring, was observed in both the spectra of pV4D4 and pD6E1-*g*-pV4D4,

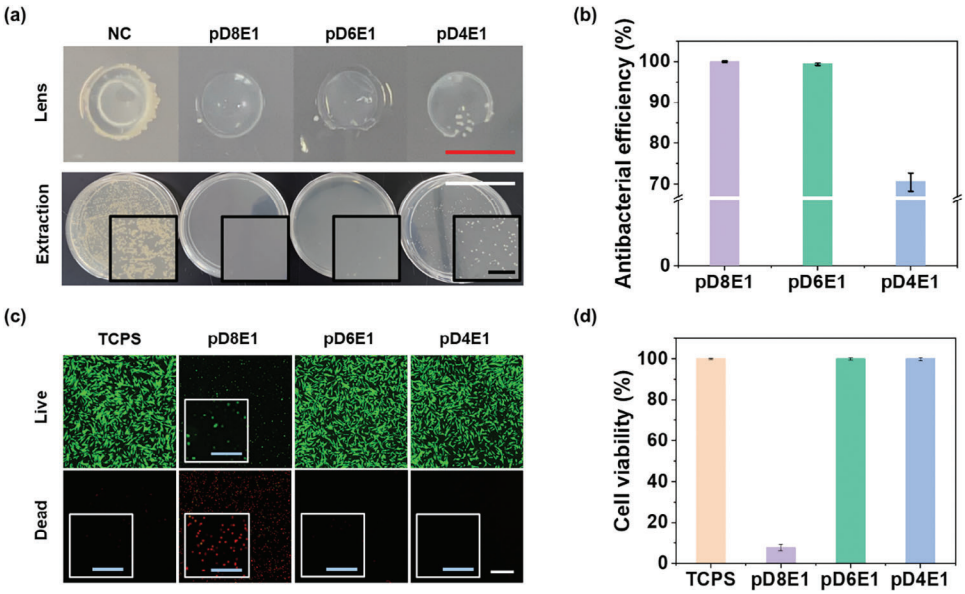

Figure 3. Antibacterial and non-cytotoxic performance of the pDE films. a) The colony assays on the extraction solution (white scale bars: 45 mm, black scale bar: 7.5 mm) in contact with pDE-coated CLs and pristine CLs (red scale bars: 10 mm) against *S. aureus* and b) the antibacterial efficiencies of the polymer surfaces. c) Live (green)/dead (red) assay of normal human dermal fibroblasts (NHDFs) cultured on the surface of pD8E1, pD6E1, and pD4E1, and tissue cultured polystyrene (TCPS) for 1 DIV. (light blue scale bars: 100 μm, white scale bars: 250 μm) d) The cell viability of thin films. Error bars indicate standard deviation ($n = 3$).

indicating the formation of pV4D4 film. The peak at 2765 cm^{-1} (highlighted in yellow), assigned to the tertiary amine in DMAMS, was observed in the spectra of both pD6E1 and pD6E1-*g*-pV4D4. These results confirmed the successful synthesis of the pD6E1-*g*-pV4D4 films via the iCVD process.

To assess the non-leaching property of the film, dishes coated with pD6E1 and pD6E1-*g*-pV4D4 were immersed in PBS solution for 2 weeks followed by gas chromatography (GC) analysis. From the GC analysis, the release of DMAMS and EGDMA moieties was clearly observed in the PBS solution from the pD6E1-coated dish, whereas no apparent peak related to DMAMS or EGDMA was observed from the pD6E1-*g*-pV4D4-coated dish. (Figure 4b; Figure S2a–d, Supporting Information). These results strongly infer that the pV4D4 adhesion promotion layer improved the adhesion of the pD6E1 layer substantially, and highlights the outstanding chemical stability of the pD6E1-*g*-pV4D4 film, which is directly linked with the long-term preservation of antibacterial performance in the PBS solution.

We further evaluated the biocompatibility of the pD6E1 film after grafting onto the pV4D4 film by introducing other types of human cells, specifically primary human corneal epithelial (HCE) cells, in addition to NHDFs.[27] As demonstrated in Figure 4c and Figure S3a,b (Supporting Information), the pD6E1-*g*-pV4D4 film showed high cell viability of over 90% for both NHDFs and HCE cells, comparable to that of TCPS,[26] confirming the excellent biocompatibility thereof.

To effectively prevent ocular diseases caused by bacteria, it is important to retain a broad spectrum of anti-bacterial properties targeting several species of bacteria. Therefore, we assessed the antibacterial properties of the pD6E1-*g*-pV4D4 film against four other bacterial species, namely *Pseudomonas. aeruginoasa* (*P. aeruginosa*), Methicillin-resistant *S. aureus* (MRSA), *Klebsiella pneumoniae* carbapenemase-producing carbapenem-resistant *Enterobacteriaceae* (KPC-CRE), and *Escherichia coli* O157: H7 (*E. coli* O157: H7). Especially, *P. aeruginosa* is one of the most common bacteria associated with bacterial keratitis and may cause permanent blindness when CLs are used improperly.[4] MRSA and KPC-CRE are each representative gram-positive and gram-negative antibiotic-resistant bacteria, respectively, and are responsible for a significant number of bacterial infections worldwide. In 2017, more than 13000 CRE infections in hospitalized patients were reported, and about 1100 deaths were caused by bacterial infections in the United States.[28] *E. coli* O157: H7 was also selected as a representative gram-negative bacteria causing severe intestinal infection in humans.[29] As shown in Figure 4d, numerous colonies were formed in the pristine dish, while no colony was observed in the pD6E1-*g*-pV4D4-coated dishes for all bacterial species. Of note, the pD6E1-*g*-pV4D4 coating enabled an antibacterial efficiency exceeding 99% against all tested species (Figure 4e). It follows from the observations above that pD6E1-g-pV4D4 exhibited exceptional antibacterial activity against a broad-spectrum of bacteria associated with ocular diseases.

The excellent antibacterial properties of the coating can be integrated monolithically into the CLs. As shown in Figure 4f, both pD6E1-g-pV4D4-coated CLs and the solution retrieved from them had completely prevented colony growth, while the pristine CLs and their solution showed significant colony growth. 6.7×10^4 colonies/CL were formed in pristine CLs, whereas the pD6E1-*g*-pV4D4-coated CLs exhibited no colonies (Figure 4g). Based on the colony assay, pD6E1-*g*-pV4D4-coated CL possessed exceptional antibacterial efficiency, with over 99.9% effectiveness (Figure S4, Supporting Information).

To investigate the optical characteristics of pDE-*g*-pV4D4 film, the transmittance of pD6E1-*g*-pV4D4 film was analyzed using

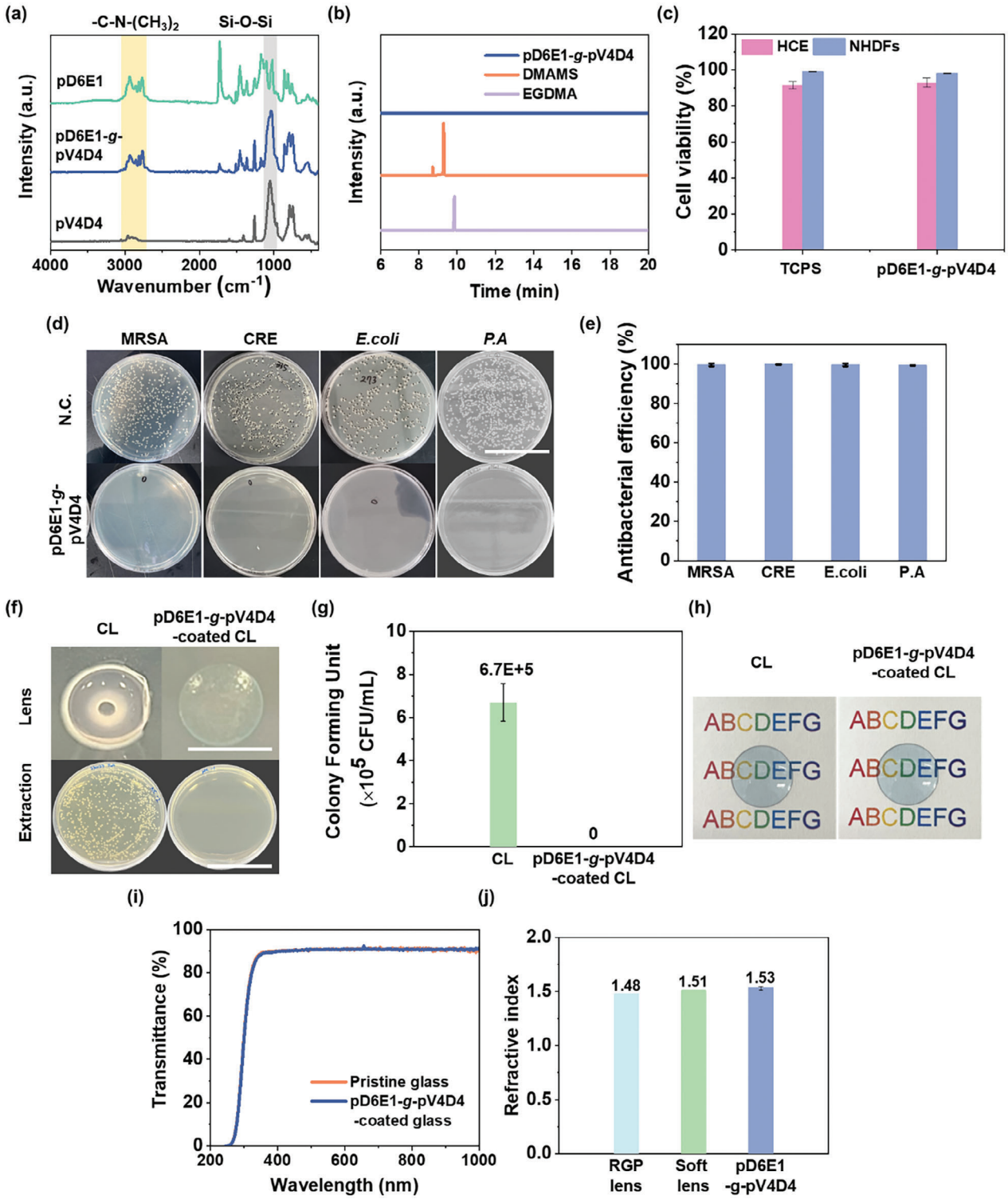

Figure 4. Characterization and antibacterial performance of pD6E1-*g*-pV4D4 film for application in CLs a) FT-IR spectra of pV4D4, pD6E1, and pD6E1-*g*-pV4D4 films, respectively ($n = 3$). b) Gas chromatography analysis data to show non-leaching property of DMAMS, EGDMA monomer, and pD6E1-g-pV4D4 thin film. c) Cell viability of pD6E1-*g*-pDV4D4 and tissue cultured polystyrene (TCPS) for 1 DIV. d) Colony assays of extraction solution (scale bars: 45 mm) in contact with pD6E1-*g*-pV4D4-coated dishes and pristine dishes (scale bars: 10 mm). e) Antibacterial efficiency of MRSA, KPC-CRE, *E. coli* O157: H7, *P. aeruginosa* in contact with the pD6E1-*g*-pV4D4 films ($n = 3$). f) Colony assays of extraction solution (scale bars: 45 mm) in contact with pD6E1-*g*-pV4D4-coated CL and pristine CL (scale bars: 10 mm) against *P. aeruginosa*. g) Corresponding antibacterial efficiencies of pD6E1-*g*-pV4D4-coated CL against *P. aeruginosa*. h) Images of pristine and pD6E1-*g*-pV4D4-coated CL between the CLs and text and i) Transmission spectra of pD6E1-*g*-pV4D4-coated glass and pristine glass. j) Refractive index of pDE-*g*-pV4D4 thin films compared to general RGP and soft lens ($n = 3$).

ellipsometry (Figure 4i), showing the full transparency of the 300 nm-thick pD6E1-*g*-pV4D4 film in whole visible light range. To confirm practical applicability, the pDE-*g*-pV4D4 film was applied to a commercially available CL, and the transparency of the pDE-*g*-pV4D4-coated CL remained unchanged (Figure 4h). Figure 4j also shows the refractive index (RI) of a rigid gas-permeable (RGP) lens, soft lens, and pD6E1-*g*-pV4D4 film, demonstrating that the RI difference of pD6E1-*g*-pV4D4 film from that of RGP and soft lenses are quite small – less than 0.05.[30] These results demonstrate that pD6E1-*g*-pV4D4 coating does not induce significant visible aberration and maintains an RI similar to that of CLs, thereby confirming the suitability of the coating for CLs. Generally, liquid-based coating processes pose significant challenges in achieving uniform ultrathin film on the non-flat surface of soft and delicate substrates like CLs while maintaining their CL integrity.[8,11h] On the other hand, the iCVD process allows for conformal ultrathin – sub-micron-thick – coating even on non-flat surfaces due to the advantages of the vapor deposition under mild process conditions, thus fully preserving optical transparency in CLs.

2.5. Long-Lasting Anti-Bacterial Properties of pD6E1-*g*-pV4D4 Film

Considering the practical duration of CL usage, it is imperative for the antibacterial coating to maintain its effectiveness over an extended period. However, only a few studies on antibacterial coatings have been reported to monitor their effectiveness over a long-term period.[11f,14,15] To date, among antibacterial coatings based on contact-killing mechanism, the longest duration of long-term antibacterial effectiveness tested is 12 weeks, however, the surface showed a substantial decrease in anti-bacterial performance with the final efficacy below 70%.[11f]

We evaluated the long-term antibacterial efficiency of synthesized pD6E1-*g*-pV4D4 against MRSA up to 9 weeks in comparison to pD6E1 films. In **Figure 5**a, the antibacterial efficiency of pD6E1 films significantly degraded by 40% only after 3 days of incubation in PBS solution (physiological conditions) and reached down to less than 30% in a 7-day incubation. On the other hand, the antibacterial performance of pD6E1-*g*-pV4D4 films was sustained for 9 weeks, retaining the antibacterial efficiency exceeding 96% during that period, which clearly confirms the long-lasting retention of the antibacterial performance of the pD6E1-*g*-pV4D4 films, attributed to the non-leaching property of the grafted pDE on pV4D4 layer that prevents the loss of antibacterial QAC moiety (Figure 4b).[11b] To the best of our knowledge, the long-term antibacterial performance retention greater than 95% surpassing 9 weeks is one of the longest ones among the QAC-based antibacterial coatings reported to date (Table S4, Supporting Information). These results strongly suggest that the unparalleled long-term preservation of antibacterial performance in the PBS solution is associated with the chemical stability of thin films, and it is of critical importance to secure a leaching-free strategy to warrant long-lasting antibacterial performance. In addition to long-lasting antibacterial performance, we compared other critical parameters, including optical properties, non-cytotoxicity, and antibacterial efficiency of the pD6E1-*g*-pV4D4 films with those of benchmark antimicrobial materials such as chitosan,[31] Ag nanoparticles,[32] and CuO nanoparticles.[33] Silver and copper oxide nanoparticles, although effective in antibacterial activity, exhibit significant cytotoxicity and poor optical transmittance, making them less suitable for contact lens applications. Chitosan, known for its biocompatibility and moderate antibacterial activity, is non-cytotoxic but has limited antibacterial durability, lasting only up to 4 days, and offers lower optical transmittance compared to pD6E1-*g*-pV4D4. In contrast, the pD6E1-*g*-pV4D4 thin film demonstrates exceptional long-lasting antibacterial performance, excellent non-cytotoxicity, and high optical transmittance, making it an ideal candidate for contact lens applications aimed at preventing ocular infections.

The mechanical durability of the pD6E1-*g*-pV4D4 film was also investigated intensively. A repeated washing cycle test was conducted to simulate the repeated usage of anti-bacterial film-coated CL. For this purpose, MRSA (1×10^4 CFU mL^{-1}) was inoculated onto the films for 2 h to check the anti-bacterial performance. Subsequently, the inoculated pD6E1-*g*-pV4D4-coated dish was rinsed with deionized water and dried in ambient air. Such a procedure was repeated and antibacterial efficiency was measured consecutively for 15 times. The results showed that the pD6E1-*g*-pV4D4 film retained greater than 99% of the initial antibacterial efficiency against MRSA (Figure 5b). Notably, the antibacterial efficiency consistently exceeded 99% across 15 consecutive cycles against MRSA. These findings confirmed the superior durability of our coating for repeated usage of CLs. To further validate the robustness of the pD6E1-*g*-pV4D4 film under conditions similar to those encountered by actual contact lens wearers, we also conducted a washing test using a 3% H_2O_2 solution, which is commonly used in many contact lens cleaning solutions. After exposure to H_2O_2, the antibacterial performance was assessed against 1×10^5 CFU mL^{-1} MRSA (Figure S5, Supporting Information). Remarkably, the pD6E1-*g*-pV4D4 film maintained over 99% antibacterial efficiency, even after multiple washing cycles with H_2O_2. Additionally, it's worth noting that while H_2O_2 is highly reactive and can impact the stability and shelf life of cleaning solutions, our thin film continued to demonstrate excellent antibacterial performance with just simple water washing. This suggests that H_2O_2 solutions may not be necessary to maintain effective antibacterial properties, offering significant advantages in terms of ease of use and longevity of the contact lenses.

To simulate harsh conditions, the pD6E1-*g*-pV4D4 film was immersed in a PBS solution containing a high concentration of salt ions in an ultrasonication bath (20 kHz) for 24 h (Figure 5c). After 24 h of ultrasonication, there was no significant change in film thickness. AFM analysis was also performed to check the change in surface morphology by measuring the root mean square roughness (RMS) value of the films before and after the 24 h ultrasonication (Figure 5d). The RMS roughness of the film remained less than 1 nm and maintained its smooth surface even after ultrasonication, indicating the mechanical robustness of the anti-bacterial coating. An anti-bacterial assay was conducted on pD6E1-*g*-pV4D4 film exposed to 4 h and 24 h of ultrasonication in PBS solution, showing the antibacterial efficiency exceeding 99% against MRSA (1×10^4 CFU mL^{-1}) for both conditions (Figure 5e). The results also confirm that the anti-bacterial films exhibit outstanding mechanical durability, enabling long-term survival in harsh physiological ocular environments.

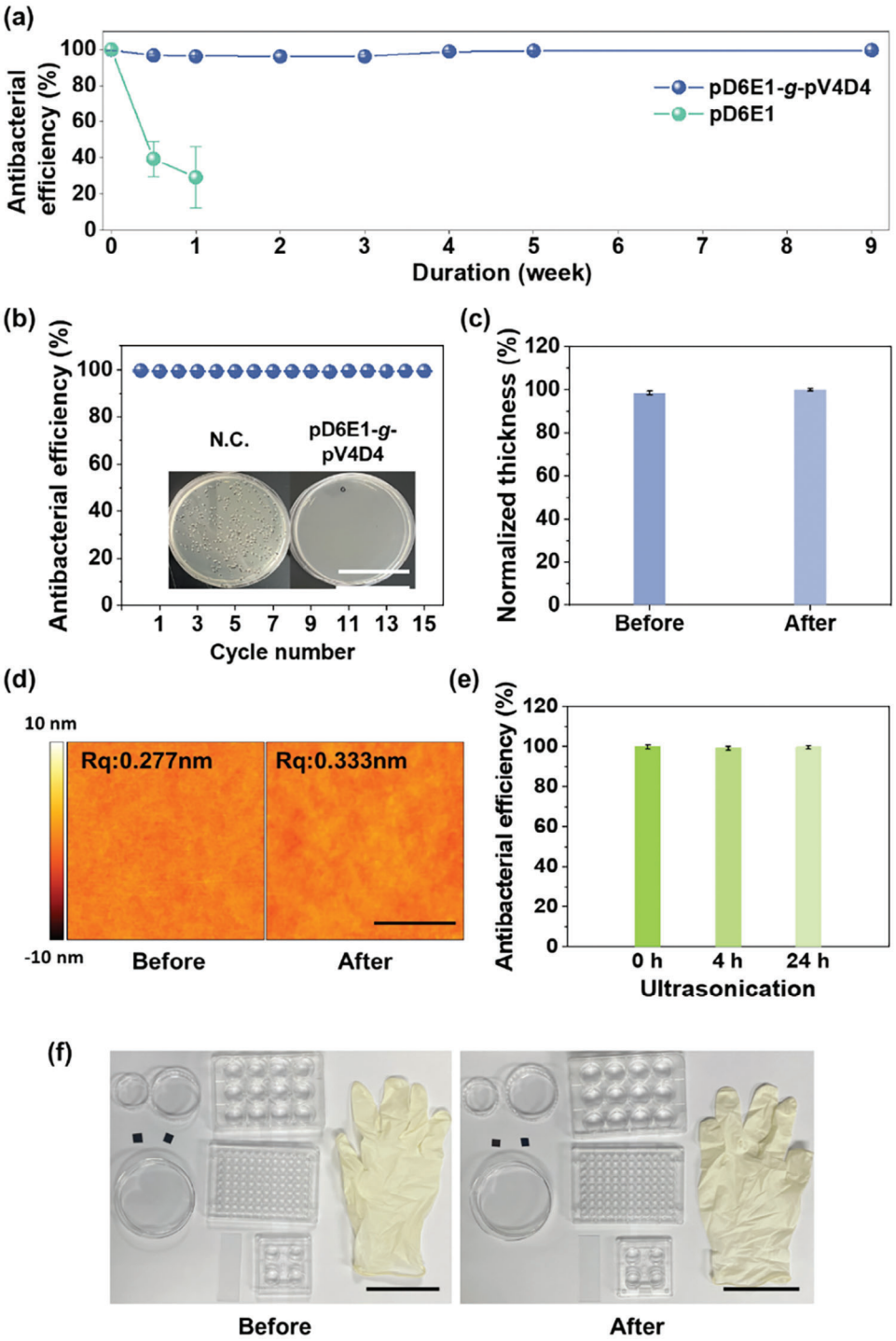

Figure 5. Chemical stability and mechanical durability of the pD6E1-*g*-pV4D4 film. For the chemical stability test, a comparison of antibacterial efficiencies of a) pD6E1 films without pV4D4 layer and pD6E1-*g*-pV4D4 films after incubation in PBS solution for an extended period against MRSA. b) Antibacterial efficiency of pD6E1-*g*-pV4D4 after 15 washing cycles against MRSA (Scale bar: 45 mm). After the ultrasonication test in PBS solution, c) thickness change, (d) AFM images of the pD6E1-*g*-pV4D4 films (Scale bar: 1 µm). e) Antibacterial efficiency of the pD6E1-*g*-pV4D4 films against MRSA after ultrasonication test in PBS solution for 4 and 24 h. f) Images of various substrates before and after iCVD coating, including a latex glove, Petri dish, cell culture plate, and Si wafers (Scale bar: 90 mm). All experiments were performed in triplicate, and the error bars represent the standard deviation.

Furthermore, the pD6E1-*g*-pV4D4 film can be applied to various substrates commonly used in the medical field, extending beyond CLs. Figure 5f depicts different substrates including a latex glove, petri dish, cell culture plate, and Si wafers before and after coating pD6E1-*g*-pV4D4 film via the iCVD process. The coated substrates show no signs of damage or color alternation post pD6E1-*g*-pV4D4 coating, indicating the formation of an ultrathin film. This highlights the versatility of the coating, as it can be effectively applied to several substrates necessitating antibacterial properties.

In our study, we assessed the wettability of the pD6E1-*g*-pV4D4 coating, which showed a water contact angle of 70°, and measured a water retention time of 1 s, both of which are important factors for the comfortability of wearing CLs (Figure S7a–c, Supporting Information). However, further investigation is necessary to comprehensively evaluate the comfortability, including additional assessments of water content, air permeability, and mechanical modulus. These aspects are critical to ensuring that the coated lenses not only provide effective antibacterial protection but also maintain the necessary comfort and breathability for long-term use.

3. Conclusion

In this study, we successfully developed a high-performance, long-lasting antibacterial coating that is non-cytotoxic and suitable for long-term, repeated use in CLs. The anti-bacterial pD6E1-*g*-pV4D4 polymer film was newly designed and synthesized using a solvent-free iCVD process. This optimized copolymer film demonstrated exceptional anti-bacterial efficiency, achieving >99% effectiveness within 2 h of exposure against various bacteria, including standard and antibiotic-resistant strains directly associated with bacterial keratitis. The introduction of the adhesion-promoting pV4D4 layer significantly enhanced the chemical stability and mechanical durability of the coating. This results in unprecedentedly superior long-lasting antibacterial performance, maintaining efficacy even after 9 weeks of incubation in PBS. The nanocoating applied under mild deposition conditions enabled the damage-free modification of the CL surface, preserving its optical properties such as transparency and refractive index comparable to pristine CLs without causing any deformation. This research highlights the potential application of the pD6E1-g-pV4D4 coating to various biomedical devices that require robust antibacterial properties. We believe that this unprecedented long-lasting anti-bacterial coating will facilitate the convenient and hygienic use of CLs, significantly reducing the risk of bacterial keratitis. Furthermore, the versatility of the iCVD process allows for the extension of this technology to a wide range of substrates and medical applications, promoting improved safety and effectiveness in healthcare settings.

4. Experimental Section

Fabrication of p(DMAMS-co-EGDMA)-g-pV4D4 Using iCVD: To synthesize pDE-*g*-pV4D4 in situ via the initiated chemical vapor deposition (iCVD) process, 1,3,5,7-tetramethyl-1,3,5,7-tetravinyl cyclotetrasiloxane (V4D4, 95%, Gelest), 2-dimethylaminomethyl styrene (DMAMS, 90%, Acros, Belgium), ethylene glycol dimethacrylate (EGMDA, 98%, Sigma–Aldrich, USA), and *tert*-butyl peroxide (TBPO, 98%, Sigma–Aldrich, USA) were heated to 70, 50, 60, and 25 °C, respectively. The vaporized monomers and initiator were injected into a customized iCVD chamber and the pDE-*g*-pV4D4 was grown directly on arbitrary substrate materials including glass, silicon wafer (Si), polystyrene (PS), rigid gas permeable (RGP) lens. The flow rate of V4D4 was 0.9 sccm. After depositing the pV4D4 thin film, pDE was deposited with the flow rates of DMAMS and EGDMA at 0.5 to 1.1 and 0.2 sccm, respectively. The chamber pressure was maintained at 150 mTorr, and the temperature of the filament was heated to 140 °C. The temperature of the substrate was 40 and 36 °C for pV4D4 and pDE, respectively.

Characterization of p(DMAMS-co-EGDMA)-g-pV4D4: To confirm the compositional ratio of thin films, Fourier transform infrared (FT-IR) spectra were obtained by using ALPHA FT-IR spectrometer in the absorbance mode (Bruker Optics) with a resolution of 1.4 cm. The composition of atomic ratio in polymer thin films was measured using an X-ray photoelectron spectrometer (Alpha K source, ThermoFisher Scientific). A spectroscopic ellipsometer (M2000, J. A. Woollam) was used to measure the thickness of the thin films. Zeta-potential values of the thin films were measured using a Nano Zetasizer 3600 (Malvern Instruments Ltd, Malvern, UK) equipped with a He-Ne laser source (633 nm). The transmittance spectra of thin films were obtained by UV/vis spectroscopy (UV-3600, Shimadzu). AFM images to measure roughness were obtained using a scanning probe microscope (NX10, Park Systems).

In Vitro Anti-Bacterial Assay: To evaluate the antibacterial activity of the thin films, the method described in ISO 22196 was implemented. *Staphylococcus aureus* (*S. aureus*, ATCC 29213), *Escherichia coli* O157: H7 (*E. coli* O157: H7, ATCC 43894), methicillin-resistant *Staphylococcus aureus* (MRSA, ATCC 43300), *Klebsiella pneumoniae* carbapenemase-producing carbapenem-resistant *Enterobacteriaceae* (KPC-CRE), *Pseudomonas. aeruginoasa* (*P. aeruginosa*, ATCC BAA-1744) were used for anti-bacterial assay. *E.coli*, *S.aureus*, *P. aeruginosa* ($\approx 1\times10^9$ CFU mL^{-1}) were cultured in Luria–Bertani (LB) broth for 24 h at 37 °C. MRSA, KPC-CRE ($\approx 1\times10^9$ CFU mL^{-1}) were cultured in Tryptic soy broth (TSB) for 24 h at 37 °C. LB agar and Tryptic soy agar (TSA) were prepared for anti-bacterial assay. 0.1 mL of bacteria ($\approx 1 \times 10^5$ CFU mL^{-1}) was spread on pDEV-coated Petri dishes (35×35 mm^2) and CLs and incubated for 2 h at room temperature. After recovering the bacterial solution in the petri dishes and CLs, 1/50 dilutions were spread on agar to count the number of viable bacteria. All experiments were in biological triplicates. The agar plates were incubated at 37 °C for more than 15 h. The anti-bacterial efficiency was calculated by the following formula:

$$\text{Anti} - \text{bacterialefficiency}\ (\%) = (1 - N/N_0) \times 100 \quad (1)$$

where N is the number of viable bacterial colonies after incubation for 2 h from the thin film-coated dishes or lens, and N_0 is the number of bacterial colonies after incubation for 2 h from non-coated dishes or lens.

Cytotoxicity Assay: Normal human dermal fibroblasts (NHDFs) purchased from Lonza (Rockland ME, USA) were selected to optimize the point between the highest cell viability and antibacterial efficiency on thin film-coated four-well cell culture plates. NHDFs were cultured in Dulbecco's Modified Eagle's Medium (DMEM, Gibco) with 10% FBS at 37 °C. 5×10^4 NHDFs were cultured on each thin film-coated and non-coated four-well cell culture plates for 1 day. After washing the culture plates with Dulbecco's phosphate-buffered saline (DPBS), and stained with a LIVE/DEAD viability/cytotoxicity kit for mammalian cells (Thermo Fisher Scientific). Each sample was incubated with DPBS (1 mL) containing ethidium homodier-1 (4 µM) solution and calcein-AM (2 µM) for 30 min at room temperature, followed by rinsing all samples with DPBS. All samples were imaged with a fluorescence microscope (Eclipse Ti-U, Nikon). Primary human corneal epithelial (HCE) cells were also cultured in corneal epithelial cell basal medium (ATCC PCS-700-030) with corneal epithelial cell growth kit (ATCC PCS-700-040) at 37 °C. HCE cells were cultured on pD6E1V coated and non-coated four-well culture plates for 1 day.

Durability Test: To evaluate the durability of thin films in an aqueous environment, similar to using CLs in the ocular environment, an ultrasonication test was performed with pD6E1-*g*-pV4D4 coating on Si wafer. In the ultrasonication test, pD6E1-*g*-pV4D4 coating on Si wafer was placed

on a petri dish and immersed in phosphate-buffered saline (PBS, Gibco). Then, the dish containing the immersed sample was placed in the ultrasonication bath with a frequency of 20 kHz. The thickness of the sample was measured using spectroscopic ellipsometer (M2000, J.A. Woollam) and exposed to ultrasonication for 24 h. AFM images were obtained using a scanning probe microscope (NX10, Park Systems) to measure the roughness of thin films after ultrasonication test. Anti-bacterial assay was performed after ultrasonication test for 4 and 24 h.

Long-Lasting Anti-Bacterial Test: A cyclic anti-bacterial assay was performed to evaluate the reuse of anti-bacterial coating for CL. In the cyclic anti-bacterial assay, 0.1 mL of bacterial solution (1×10^4 CFU mL^{-1}) was inoculated on pD6E1-*g*-pV4D4 coated and non-coated Petri dishes, followed by recovering the bacterial solution and washing the Petri dishes three times with deionized water. The recovery solution was used for an anti-bacterial assay. The cyclic anti-bacterial assay was performed using the washed dishes. To evaluate the long-lasting anti-bacterial activity of thin films, pD6E1V-coated Petri dishes were immersed in PBS to make a similar environment within the eyes. After removing the PBS solution, the Petri dishes were washed three times with deionized water and dried with an air gun. Then, an anti-bacterial assay was performed until 9 weeks after immersing the dishes in PBS.

Statistical Analysis: Statistical analyses were performed using OriginPro 2019 (OriginLab Corporation, Northampton, USA). Data points represent the mean of at least three independent measurements. Sample size (n) for each statistical analysis is three ($n = 3$).

Supporting Information

Supporting Information is available from the Wiley Online Library or from the author.

Acknowledgements

This work was supported by the Nanomedical Devices Development Project of NNFC 2024, by the Commercialization Promotion Agency for R&D Outcomes(COMPA) funded by the Ministry of Science and ICT(MSIT)(No. 2710006589), and by 2024 Innovation Technology Advancement and Commercialization Suppot Project funded by Startup KAIST and Daejeon Metropolitan City. This research was also supported by the National Research Foundation of Korea (NRF) grant funded by the Korean government (Ministry of Science and ICT) (No.2022M3H4A4085936, RS-2023-00302611, RS-2024-00438316, and RS-2024-00439931).

Conflict of Interest

The authors declare no conflict of interest.

Author Contributions

N.P., C.-E.M., and Y.S. contributed equally to this work. N.P., M.C.E., and Y.S. conceived the original idea. K.G.L., Y.W.J., and S.G.I proposed the research. N.P. and Y.S. designed the schematic illustration and performed iCVD coating and material analysis. S.S conducted AFM and XPS measurements. S.Y., S.P., and J.Y. conducted a cytotoxicity assay. C.E.M, J.M.K., and J.L. performed an anti-bacterial assay against *Pseudomonas Aeruginosa*. B.J. conducted FT-IR measurements. All authors discussed and analyzed the data. N.P., C.E.M., and Y.S. contributed to the writing and revision of the manuscript. K.G.L., Y.W.J., and S.G.I procured the funding, supervised the project, and reviewed and refined the manuscript.

Data Availability Statement

The data that support the findings of this study are available from the corresponding author upon reasonable request.

Keywords

broad-spectrum anti-bacterial, contact lens, initiated chemical vapor deposition (iCVD), long-lasting anti-bacterial, transparency

Received: July 7, 2024
Revised: September 19, 2024
Published online: September 30, 2024

[1] a) S. A. Khan, S. Shahid, T. Mahmood, C.-S. Lee, *Acta Biomater.* **2021**, *128*, 262; b) Z. Jiao, Q. Huo, X. Lin, X. Chu, Z. Deng, H. Guo, Y. Peng, S. Lu, X. Zhou, X. Wang, B. Wang, *Carbohydr. Polym.* **2022**, *286*, 119314; c) H.-Y. Lin, S.-W. Wang, J.-Y. Mao, H.-T. Chang, S. G. Harroun, H.-J. Lin, C.-C. Huang, J.-Y. Lai, *Chem. Eng. J.* **2021**, *411*, 128469.

[2] a) R. Lace, K. G. Doherty, D. Dutta, M. D. P. Willcox, R. L. Williams, *Adv. Mater. Interfaces* **2020**, *7*, 2001232; b) C. N. Ezisi, C. E. Ogbonnaya, O. Okoye, E. Ezeanosike, H. Ginger-Eke, O. C. Arinze, *Nigerian J. Ophthalmology* **2019**, *26*, 1.

[3] M. P. Brynildsen, J. A. Winkler, C. S. Spina, I. C. MacDonald, J. J. Collins, *Nat. Biotechnol.* **2013**, *31*, 160.

[4] Y. Hilliam, S. Kaye, C. Winstanley, *J. Med. Microbio.* **2020**, *69*, 3.

[5] J. W. Lee, T. Somerville, S. B. Kaye, V. Romano, *J. Clin. Med.* **2021**, *10*, 758.

[6] F. Stapleton, L. Keay, K. Edwards, T. Naduvilath, J. K. Dart, G. Brian, B. A. Holden, *Ophthalmology* **2008**, *115*, 1655.

[7] a) L. Zhou, C. Zhao, W. Yang, *Colloids Surf., B* **2022**, *217*, 112710; b) O. Girshevitz, Y. Nitzan, C. N. Sukenik, *Chem. Mater.* **2008**, *20*, 1390; c) C. Zhao, L. Zhou, M. Chiao, W. Yang, *Adv. Colloid. Interface Sci.* **2020**, *285*, 102280.

[8] H. Yazdani-Ahmadabadi, D. F. Felix, K. Yu, H. H. Yeh, H. D. Luo, S. Khoddami, L. E. Takeuchi, A. Alzahrani, S. Abbina, Y. Mei, L. Fazli, D. Grecov, D. Lange, J. N. Kizhakkedathu, *ACS Cent. Sci.* **2022**, *8*, 546.

[9] R. Bright, D. Fernandes, J. Wood, D. Palms, A. Burzava, N. Ninan, T. Brown, D. Barker, K. Vasilev, *Mater. Today Bio.* **2022**, *13*, 100176.

[10] G. Choi, G. M. Jeong, M. S. Oh, M. Joo, S. G. Im, K. J. Jeong, E. Lee, *ACS Biomater. Sci. Eng.* **2018**, *4*, 2614.

[11] a) X. Nie, S. Wu, F. Huang, W. Li, H. Qiao, Q. Wang, Q. Wei, *Chem. Eng. J.* **2021**, *416*, 129072; b) J. Huang, Y. Cao, S. Ding, *Biomaterials* **2023**, *301*, 122214; c) M. Fan, J. Si, X. Xu, L. Chen, J. Chen, C. Yang, J. Zhu, L. Wu, J. Tian, X. Chen, X. Mou, X. Cai, *Carbohydr. Polym.* **2021**, *257*, 117636; d) H. Li, Y. Li, Y. Wang, L. Liu, H. Dong, T. Satoh, *Acta Biomater.* **2022**, *142*, 136; e) Y. Li, Y. Miao, L. Yang, G. Wang, M. Fu, Y. Wang, D. Fu, J. Huang, J. Wang, Z. Fan, Z. Lu, J. Guo, Z. Hu, *Chem. Eng. J.* **2023**, *455*, 140572; f) R. Lin, Z. Wang, Z. Li, L. Gu, *Mater. Today Bio.* **2022**, *15*, 100330; g) Z. Huang, S. Nazifi, A. Hakimian, R. Firuznia, H. Ghasemi, *ACS Appl. Mater. Interfac.* **2022**, *14*, 43681; h) W. Li, Y. Wang, Y. Qi, D. Zhong, T. Xie, K. Yao, S. Yang, M. Zhou, *ACS Appl. Bio Mater.* **2021**, *4*, 3729; i) Q. Yao, J. Zhang, G. Pan, B. Chen, *ACS Appl. Mater. Interfac.* **2022**, *14*, 36473; j) V. Gribova, F. Boulmedais, A. Dupret-Bories, C. Calligaro, B. Senger, N. E. Vrana, P. Lavalle, *ACS Appl. Mater. Interfac.* **2020**, *12*, 19258; k) Y. Wang, K. Ma, J. Bai, T. Xu, W. Han, C. Wang, Z. Chen, K. O. Kirlikovali, P. Li, J. Xiao, O. K. Farha, *Angew. Chem., Int. Ed.* **2022**, *61*, e202115956; l) S. Wu, J. Xu, L. Zou, S. Luo, R. Yao, B. Zheng, G. Liang, D. Wu, Y. Li, *Nat. Commun.* **2021**, *12*, 3303.

[12] P. Liu, Y. Wu, B. Mehrjou, K. Tang, G. Wang, P. K. Chu, *Adv. Funct. Mater.* **2022**, *32*, 2110635.

[13] H. Van Acker, T. Coenye, *Trends Microbiol.* **2017**, *25*, 456.

[14] P. Krys, H. Schroeder, J. Buback, M. Buback, K. Matyjaszewski, *Macromolecules* **2016**, *49*, 7793.

[15] T.-W. Huang, Y.-C. Ho, T.-N. Tsai, C.-L. Tseng, C. Lin, F.-L. Mi, *Carbohydr. Polym.* **2020**, *242*, 116312.
[16] a) S. J. Yu, K. Pak, M. J. Kwak, M. Joo, B. J. Kim, M. S. Oh, J. Baek, H. Park, G. Choi, D. H. Kim, J. Choi, Y. Choi, J. Shin, H. Moon, E. Lee, S. G. Im, *Adv. Eng. Mater.* **2018**, *20*, 1700622; b) Y. Choi, Y. T. Kim, S. J. Lee, E. Lee, K. G. Lee, S. G. Im, *Macromol. Res.* **2020**, *28*, 249; c) K. K. Gleason, *Adv. Mater.* **2023**, *36*, 2306665; d) G. Choi, Y. Song, H. Lim, S. H. Lee, H. K. Lee, E. Lee, B. G. Choi, J. J. Lee, S. G. Im, K. G. Lee, *Adv. Healthcare Mater.* **2020**, *9*, 2000447.
[17] a) M. A. Gelman, B. Weisblum, D. M. Lynn, S. H. Gellman, *Org. Lett.* **2004**, *6*, 557; b) Y. Song, Y. T. Kim, Y. Choi, H. Kim, M. H. Yeom, Y. Kim, T. J. Lee, K. G. Lee, S. G. Im, *Adv. Healthcare Mater.* **2021**, *10*, 2100430; c) Q. Song, R. Zhao, T. Liu, L. Gao, C. Su, Y. Ye, S. Y. Chan, X. Liu, K. Wang, P. Li, W. Huang, *Chem. Eng. J.* **2021**, *418*, 129368.
[18] H. Kim, Y. Song, S. Park, Y. Kim, H. Mun, J. Kim, S. Kim, K. G. Lee, S. G. Im, *Adv. Funct. Mater.* **2022**, *32*, 2113253.
[19] a) Y. Yoo, J. B. You, W. Choi, S. G. Im, *Polym. Chem.* **2013**, *4*, 1664; b) R. Chen, Y. Zhang, Q. Xie, Z. Chen, C. Ma, G. Zhang, *Adv. Funct. Mater.* **2021**, *31*, 2011145; c) D. J. Wilson, D. H. Chenery, H. K. Bowring, K. Wilson, R. Turner, J. Maughan, P. J. West, C. W. Ansell, *J. Biomater. Sci., Polym. Ed.* **2005**, *16*, 449.
[20] Y. Song, Y.-k. Lee, Y. Lee, W.-T. Hwang, J. Lee, S. Park, N. Park, H. Song, H. Kim, K. G. Lee, I.-D. Kim, Y. Kim, S. G. Im, *Chem. Eng. J.* **2023**, *470*, 144224.
[21] Q. Song, S. Y. Chan, Z. Xiao, R. Zhao, Y. Zhang, X. Chen, T. Liu, Y. Yan, B. Zhang, F. Han, P. Li, *Prog. Org. Coat.* **2024**, *188*, 108214.
[22] G. Choi, Y. Cho, S. J. Yu, J. Baek, M. Lee, Y. Kim, E. Lee, S. G. Im, *ACS Appl. Bio Mater.* **2020**, *3*, 7654.
[23] M. Malani, A. T. Thodikayil, S. Saha, J. Nirmal, *Carbohydr. Polym.* **2024**, *324*, 121558.
[24] C. Intini, L. Elviri, J. Cabral, S. Mros, C. Bergonzi, A. Bianchera, L. Flammini, P. Govoni, E. Barocelli, R. Bettini, M. McConnell, *Carbohydr. Polym.* **2018**, *199*, 593.
[25] N. Lewinski, V. Colvin, R. Drezek, *Small* **2008**, *4*, 26.
[26] R. F. Wallin, E. Arscott, *Med. Dev. Diagn. Ind.* **1998**, *20*, 96.
[27] J. Aveyard, R. C. Deller, R. Lace, R. L. Williams, S. B. Kaye, K. N. Kolegraff, J. M. Curran, R. A. D'Sa, *ACS Appl. Mater. Interfaces* **2019**, *11*, 37491.
[28] Centers for Disease Control and Prevention, About Carbapenem-resistant Enterobacterales, https://www.cdc.gov/cre/about/index.html, (accessed: September 2024).
[29] X. Wei, J. Li, S. Hou, C. Xu, H. Zhang, E. R. Atwill, X. Li, Z. Yang, S. Chen, *Int. J. Envir. Res. Publ. Health* **2018**, *15*, 1416.
[30] a) H. M. Reinhardt, D. Recktenwald, H.-C. Kim, N. A. Hampp, *J. Mater. Sci.* **2016**, *51*, 9971; b) M. intergroup, RGP Lens, https://www.marshalintergroup.com/_files/ugd/830fec_1f5e76ba80f64530ad2a1d8927275b65.pdf, (accessed: September 2024).
[31] a) J. Li, Y. Wu, L. Zhao, *Carbohydr. Polym.* **2016**, *148*, 200; b) A. M. Piras, G. Maisetta, S. Sandreschi, M. Gazzarri, C. Bartoli, L. Grassi, S. Esin, F. Chiellini, G. Batoni, *Front. Microbiol.* **2015**, *6*, 372; c) S. C. Fernandes, C. S. Freire, A. J. Silvestre, C. Pascoal Neto, A. Gandini, L. A. Berglund, L. Salmén, *Carbohydr. Polym.* **2010**, *81*, 394.
[32] a) B. S. Fazly Bazzaz, B. Khameneh, M.-m. Jalili-Behabadi, B. Malaekeh-Nikouei, S. A. Mohajeri, *Cont. Lens Anter. Eye* **2014**, *37*, 149; b) M. Wu, S. Yu, L. He, L. Yang, W. Zhang, *Sci. Rep.* **2017**, *7*, 103; c) B. Demir, R. M. Broughton, M. Qiao, T. S. Huang, S. D. Worley, *Molecules* **2017**, *22*, 1582.
[33] a) R. Daira, A. Kabir, B. Boudjema, C. Sedrati, *Solid State Sci.* **2020**, *104*, 106254; b) R. Rajamma, S. Gopalakrishnan Nair, F. Abdul Khadar, B. Baskaran, *IET Nanobiotechnol* **2020**, *14*, 833; c) A. Yoosefi Booshehri, R. Wang, R. Xu, *Chem. Eng. J.* **2015**, *262*, 999; d) L. L. Duffy, M. J. Osmond-McLeod, J. Judy, T. King, *Food Control* **2018**, *92*, 293.